https://doi.org/10.1038/s44355-024-00007-7

# Stiffness-induced modulation of ERG transcription factor in chronic liver disease



Sonia-Emilia Selicean[1,2,5], Eric Felli[1,2,5], Cong Wang[1,2], Yeldos Nulan[1,2], Juan José Lozano[3], Sergi Guixé-Muntet[3], Horia Ștefănescu[4], Jaime Bosch[1,2,3], Annalisa Berzigotti[1,2] & Jordi Gracia-Sancho[1,2,3] ✉

Chronic liver disease (CLD) is characterised by liver sinusoidal endothelial cells (LSECs) dysfunction. Mechanical forces and inflammation are among the leading factors. ETS-related gene (ERG) is an endothelial-specific transcription factor, involved in maintaining cell quiescence and homeostasis. Our study aimed to understand the expression and modulation of ERG in CLD. ERG expression was characterised and correlated to clinical data in human liver cirrhosis at different disease stages. ERG dynamics in response to stiffness and inflammation were investigated in primary healthy and cirrhotic rat LSEC and in human umbilical vein endothelial cells (HUVECs). ERG is markedly downregulated in cirrhosis independently of disease stage or aetiology and its expression is modulated by substrate stiffness in ECs. Inflammation downregulates ERG in cells on physiological stiffness, but not on high stiffness, suggesting a complementary role of inflammation and stiffness in suppressing ERG. This study outlines ERG as an LSEC inflammation and stiffness-responsive transcription factor in cirrhosis.

Cirrhosis of the liver is the final stage of CLD and is characterized by marked changes in liver structure and function due to extensive fibrosis, parenchymal extinction, and nodular regeneration. A major consequence of cirrhosis is the development of portal hypertension (PH), responsible for its complications and for the need of liver transplantation. LSECs play a crucial role in the development and progression of cirrhosis and PH. Indeed, in response to liver injury and pro-inflammatory stimuli, LSECs become dedifferentiated, acquiring a proinflammatory, profibrotic and coagulation-prone phenotype[1,2]. Recently, attention has shifted to the important influence of mechanical forces in the progression of CLD and portal hypertension (PH)[3]. Among these forces, it has been shown that LSECs phenotype can be modulated by increased tissue stiffness, as it is encountered in cirrhosis of the liver. Healthy LSECs exposed to stiff substrates dedifferentiate and become dysfunctional and pseudo-capillarized. In contrast, soft substrates partially ameliorate cirrhotic LSECs dysfunction[4]. Moreover, increased tissue stiffness impacts the inflammatory response of LSECs by modulating nuclear factor kappa B (NFkB) localization and chemokine ligand 1 (CXCL1) expression[5]. Studies in other EC types confirmed the link between stiffness and inflammation[6,7]. At the nuclear level, mechanical forces can influence the expression of transcription factors (TFs) and co-factors[8]. One such example is Krüppel-like factor 2 (KLF2), which is modulated by shear stress in LSECs and plays a vasoprotective and anti-fibrotic role during the development of CLD[9–12]. Tissue stiffness has also been demonstrated to modulate the localization and activity of transcription cofactors, among which YAP/TAZ[13] and MRTF-A[14]. Whether other endothelial TFs are modulated by mechanical forces in liver injury is so far unexplored. The transcription factor ETS-related gene (ERG) is an endothelial-specific TF in the post-developmental phase that belongs to the ETS family[15]. Furthermore, it acts as an oncogene in tissues such as the prostate[16] and white blood cells[17]. ERG contributes to the maintenance of vascular homeostasis through its anti-inflammatory[18–20] and anti-thrombotic[21] functions, as well as by maintaining normal endothelial barrier integrity and regulating angiogenesis[22,23]. Recently, ERG has been involved in lung pathophysiology[24–27] and in liver disease[28], where it was shown to prevent endothelial-to-mesenchymal transition during the development of CLD[28]. Several ERG modulation pathways have been described, such as those related to ubiquitination[27,29,30] or miRNAs in prostate cancer or ERG phosphorylation in the endothelium[31], however, the mechanisms leading to ERG downregulation in lung or liver disease remain elusive. The aim of this study was to investigate ERG dynamics over the

[1]Department of Visceral Surgery and Medicine, Inselspital, Bern University Hospital, University of Bern, Bern, Switzerland. [2]Department for BioMedical Research, Visceral Surgery and Medicine, University of Bern, Bern, Switzerland. [3]Liver Vascular Biology Research Group, IDIBAPS Biomedical Research Institute, CIBER-EHD, University of Barcelona, Barcelona, Spain. [4]Liver Unit, Regional Institute of Gastroenterology and Hepatology Octavian Fodor, Cluj-Napoca, Romania. [5]These authors contributed equally: Sonia-Emilia Selicean, Eric Felli. ✉e-mail: jgracia@recerca.clinic.cat

course of CLD, as well as unveil possible mechanisms related to its downregulation.

## Results

### ERG is a potential mechanosensitive factor involved in advanced chronic liver disease

ERG expression was significantly downregulated in our previously published human healthy vs cirrhotic transcriptomic dataset[32], being the most significantly differentially expressed transcription factor (log2FC = −6.68; *p*-value = 0.005; GSE164799). Indeed, this downregulation was confirmed at the protein level by IF in a small cohort of patients without cirrhosis ($n = 11$) vs patients with cirrhosis ($n = 12$) (Fig. 1A, B). Supplementary Table 1 shows demographic characteristics and standard liver tests of the cohort of patients with cirrhosis.

To better understand the possible roles of ERG in ECs, we first took advantage of the ARCHS[4] RNA-Seq gene-gene co-expression matrix and identified the top 200 ERG co-expressed genes (full list in Supplementary Table 2). Pathway analysis revealed that ERG-dependent genes are related to processes involved in angiogenesis (P00005) and inflammation (P00031), as previously described in other studies. Interestingly, integrin signaling (P00034) was found among the top represented pathways, suggesting that ERG may be involved in processes related to mechanobiology, as integrins are a crucial part of the mechanoresponsive machinery of cells (Supplementary Table 3). Enrichr-KG analysis of the pre-expanded gene list further suggested a possible involvement of ERG in ECM organization (Fig. 2A, B). Next, to narrow down the question to the role of ERG in ECs, we used two publicly available RNA sequencing databases of ERG knock down in HUVECs, GSE18401 and GSE32984. Gene set enrichment analysis of these two datasets revealed that loss of ERG has a major influence on the upregulation of inflammatory pathways (Fig. 2C, D), as previously described[18,20]. Moreover, overrepresentation analysis of the differentially expressed genes (DEGs) (FC ± 1.5, $p < 0.05$) in both datasets similarly revealed ERG involvement in inflammation and in integrin signaling (P00034) (Supplementary Tables 4 and 5). To better understand the possible roles of ERG in CLD, we compared our previously published RNA Sequencing dataset obtained from cirrhotic versus healthy human LSECs (hLSECs) (GSE164799) with the two publicly available datasets of ERG knockdown HUVECs (GSE18401 and GSE32984). DEGs from the three datasets were selected using the thresholds of FC ± 1.5 and $p < 0.05$ and common DEGs were selected. Comparison with GSE18401 identified 155 (9.81%) common DEGs (Fig. 2E, F) and comparison with GSE32984 identified 49 (3.2%) common DEGs (Supplementary Fig. 1A, B). Functional pathways classification of the common DEGs between hLSECs and GSE18401, revealed integrin signaling (P00034), inflammation (P00036 and P00031) and angiogenesis (P0005 and P00056) among the most represented (Fig. 2G). Moreover, GO pathway analysis classified the common DEGs into pathways involved in angiogenesis and cell adhesion (Fig. 2H). Similarly, common DEGs between hLSECs and GSE32984 also showed involvement in pathways related to inflammation and angiogenesis, confirming the involvement of ERG in these processes during the development of CLD (Supplementary Fig. 1C, D). Overall, these analyses support an important role of ERG in inflammation and angiogenesis, as well as a possible role in pathways related to mechanobiology.

### ERG expression is modulated by matrix stiffness and inflammatory stimuli

The possible connection between ERG and mechanobiology was investigated in experiments assessing whether matrix stiffness may contribute to ERG downregulation in CLD. Furthermore, to understand the interplay between substrate stiffness and inflammation on ERG modulation, we assessed the role of IL1β in this context. HUVECs were seeded on collagen-I coated PAA gels of 0.5 and 30 kPa for 72 h and treated with 10 ng/mL IL1β or vehicle for an additional 24 h. Both immunofluorescence and WB demonstrated a significant downregulation of ERG in response to high stiffness (30 kPa) PAA gel (Fig. 3A, B). Moreover, IL1β also resulted in ERG downregulation at 0.5 kPa, but no further downregulation was observed at 30 kPa when compared to the vehicle-treated control (Fig. 3A, B). qRT-PCR did not show differences in ERG mRNA expression neither in response to increased stiffness (Fig. 3C), suggesting the mechanism for the observed ERG downregulation involved a posttranslational degradation, as already described for inflammatory stimuli[27]. To more precisely address if these alterations are specifically observed in the liver, we assessed the response of freshly isolated rat LSECs to 24 h exposure to increased stiffness. The rationale behind the longer culture time in HUVEC compared to LSECs stands in the fact that cells previously expanded on polystyrene tissue culture plates may require a longer adaptation time to softer substrates, possibly due to stiffness-induced epigenetic changes (as shown in[33,34] and by our unpublished observations). In LSECs isolated from healthy livers, ERG protein expression was consistently downregulated when cultured in the 30 kPa PAA substrate (Fig. 3D). Conversely, cirrhotic rat LSECs showed a trend towards recovery of ERG expression when cultured under soft substrate conditions. Of note, the response was of similar magnitude as that observed in healthy rat LSECs on 30 kPa (Fig. 3E).

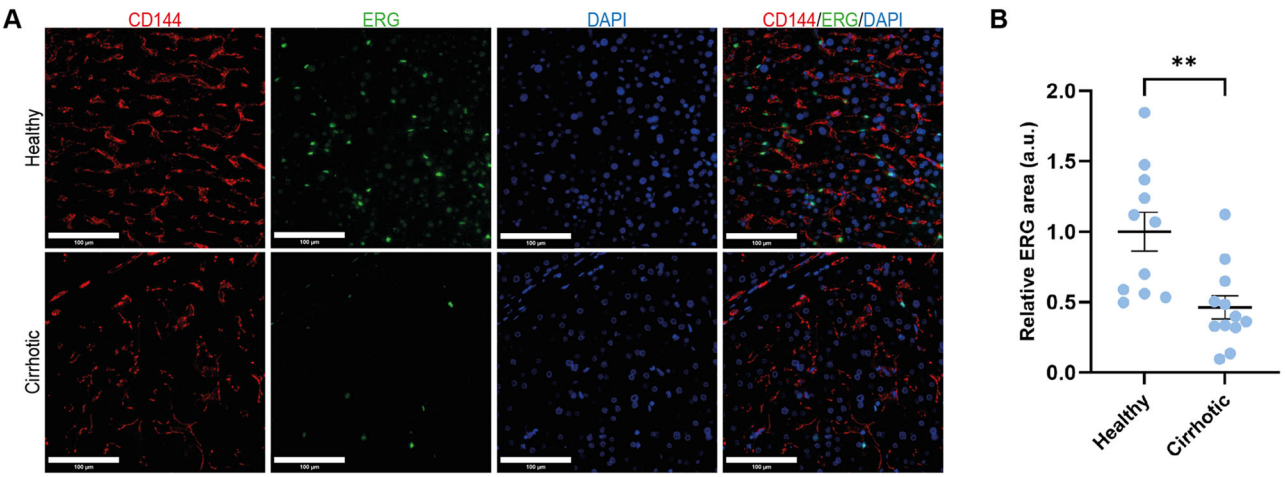


**Fig. 1 | ERG is downregulated in advanced chronic liver disease. A** IF and **B** corresponding quantification of ERG (green) expression in human healthy and cirrhotic liver tissue from two independent cohorts of patients. CD144 (red) was used as marker for ECs. For each experiment, sample distributions were assessed for normality (Kolmogorov-Smirnov test). Normally distributed data were compared with unpaired Student t test ** = $p \leq 0.01$. CD144=cluster of differentiation 144, DAPI = 4′,6-diamidino-2-phenylindole, scale bar = 100 um.

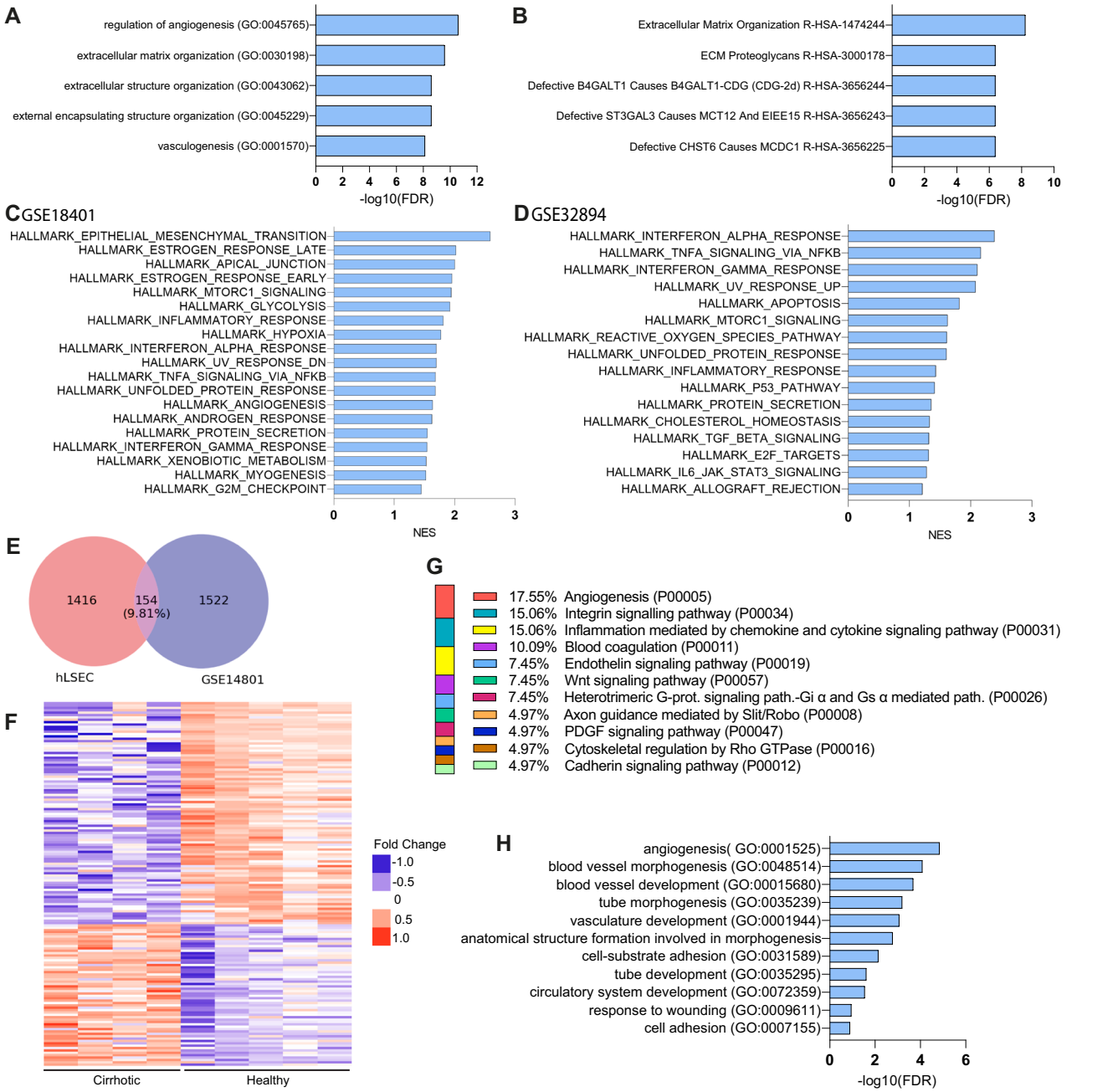


**Fig. 2 | ERG is involved in inflammation, angiogenesis and mechanobiology response. A**, **B** Enrichr-KG analysis of the pre-expanded top 200 ERG co-expressed genes: **A** Gene Ontology process (GO), **B** Reactome. **C**, **D** Hallmarks obtained by GSEA analysis of HUVEC ERG knock-down databases GSE14801 and GSE32984, respectively. **E** Venn diagram showing the intersection between hLSEC (GSE164799) and GSE14801. **F** Heatmap of common DEGs between hLSEC (GSE164799) and GSE14801, as expressed in healthy vs cirrhotic human LSECs. **G** Panther pathway analysis of the common DEGs. **H** GO pathway analysis of the common DEGs.

## ERG is downregulated in patients with cirrhosis and in rats with experimental cirrhosis

Due to the fact that ERG is modulated by stiffness and inflammation, we next decided to extend our human study by including a larger cohort of patients with cirrhosis ($n = 29$) (Table 1) in different disease stages, represented by increasing liver stiffness and increased inflammation: compensated cirrhosis ($n = 9$), decompensated cirrhosis presenting with 1 decompensation ($n = 10$) or decompensated cirrhosis presenting with more than 1 decompensation ($n = 10$). Any of the following clinical events were considered as decompensation: development of ascites, variceal hemorrhage, hepatic encephalopathy, or hepato-renal syndrome. Etiology of cirrhosis was viral in 44% of the patients, followed by autoimmune – AIH, PBC or PSC (28%), ARLD (17%) and MASH (10%). The majority (90%) of the patients had clinically significant portal hypertension, defined by a hepatic vein pressure gradient (HVPG) ≥ 10 mmHg. ERG expression was similar across stages of advanced liver disease (Fig. 4A, B) and its levels were also independent of disease etiology (Fig. 4C). Furthermore, ERG expression did not show a correlation with any of the clinical variables investigated, except for a weak negative correlation with ALT levels ($r = -0.37$, $p = 0.04$). There was no correlation between ERG protein levels and in vivo liver stiffness values, as measured by Vibration Controlled Transient Elastography ($r = -0.25$, $p = 0.29$).

We further assessed ERG expression in rat livers during the progression of $CCl_4$-induced cirrhosis at 2 weeks ($n = 4$), 6 weeks ($n = 5$), full

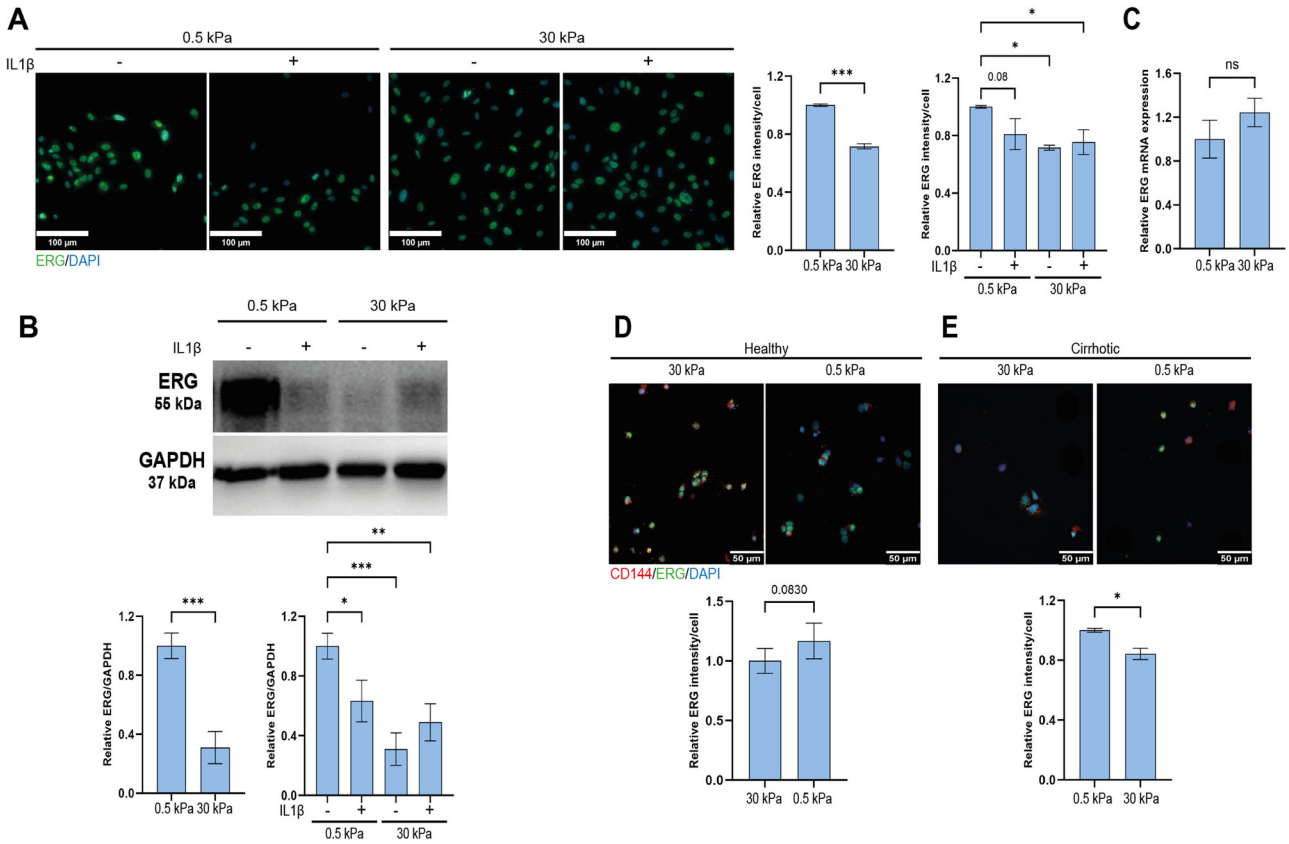


**Fig. 3 | ERG is downregulated in response to high stiffness and inflammation.** **A** Representative IF images and quantification of ERG (green) in HUVECs seeded for 72 h on 0.5 vs 30 kPa PAA gels and treated for an additional 24 h with IL1b or vehicle ($n = 969$ cells from 0.5 kPa, $n = 744$ cells from 0.5 kPa IL1β, $n = 1132$ cell from 30 kPa and $n = 1133$ cells from 30 kPa IL1β, from $n = 3$ independent experiments). **B** Representative Western Blot in HUVECs seeded for 72 h on 0.5 vs 30 kPa PAA gels and treated for an additional 24 h with IL1b or vehicle. ERG expression was normalized to GAPDH as housekeeping protein ($n = 6$ independent experiments - Supplementary Fig. 3). **C** qRT-PCR of ERG gene in HUVECs seeded for 96 h of 0.5 vs 30 kPa ($n = 3$ independent experiments). **D** Representative IF images and quantification of ERG in freshly isolated healthy rat LSECs seeded on 0.5 vs 30 kPa PAA gels for 24 h ($n = 120$ cells from 0.5 kPa and $n = 144$ cells from 30 kPa were analysed, from $n = 4$ rats). **E** Representative IF images and quantification of ERG in freshly isolated cirrhotic rat LSECs seeded on 0.5 vs 30 kPa PAA gels for 24 h ($n = 78$ cells from 0.5 kPa and $n = 178$ cells from 30 kPa were analysed, from $n = 3$ rats). All IF data were normalized to the number of cells. For each experiment, sample distribution was assessed for normality (Kolmogorov-Smirnov test). Normally distributed data were compared with unpaired Student t test, otherwise with Mann-Whitney test. Data for the stiffness + inflammation comparison were normalized to the 0.5 kPa vehicle condition and analyzed with Ordinary One-way ANOVA, * = $p < 0.05$; ** = $p \leq 0.01$; *** = $p \leq 0.001$, scale bar HUVEC = 100 µm, scale bar LSEC = 50 µm.

cirrhosis ($n = 5$), as well as after 8 weeks of stopping TAA administration (spontaneous regression) ($n = 5$) and compared it to healthy rat tissue ($n = 5$). There was no difference in ERG protein expression during progression of the disease before cirrhosis development, and significant but moderate downregulation in the fully cirrhotic stage, compared to the healthy rats. After 8 weeks of spontaneous regression[32], ERG expression returned to baseline levels (Supplementary Fig. 2).

## Discussion

In this paper, we investigated the ERG transcription factor, which is downregulated in cirrhosis, as previously demonstrated by Dufton et al.[28] and confirmed by our transcriptomic and IF data. Following this, we tried to gain a better insight on the possible role of ERG in the pathophysiology of liver disease, by comparing publicly available ERG knock-down transcriptomics datasets with our human healthy vs cirrhosis dataset. Commonly deregulated pathways seem to be involved mostly in pathways related to vascular development and angiogenesis via Notch and Wnt signaling[15], which, intrahepatically, are intimately connected to fibrogenic processes in liver pathobiology[35,36]. Moreover, by pathway analysis, we observed a possible novel relationship between ERG and mechanobiology, since loss of ERG affected genes related to integrin signaling. This connection is in line with previously described involvement of ERG in modulating microtubule dynamics and EC migration[22,23]. Indeed, we demonstrated both in HUVECs and freshly isolated LSECs that ERG is downregulated in response to increased substrate stiffness, as found in cirrhotic livers. In our study, we confirmed that ERG is regulated by inflammatory stimuli[18]. This may occur due to the inhibition of NF-κB p65 binding to the promoters of pro-inflammatory genes[18,20]. Additionally, ERG responds to mechanical forces, such as high and low shear stress, by directly modulating thrombomodulin and indirectly by facilitating chromatin access to Krüppel-like Factor 2 (KLF2), a key regulator of nitric oxide release, to the thrombomodulin promoter[21].

It is well known that liver stiffness measurements (LSM) have prognostic value in cirrhosis. This has been particularly well demonstrated using transient elastography, to the point that the recent Baveno guidelines for prognostic stratification include the use of LSM[37]. In addition, progression, and regression of cirrhosis are paralleled by increasing respectively decreasing LSM values[38]. The increased liver stiffness in cirrhosis is mainly due to fibrosis, but it is also increased by inflammation[39,40]. It is worth noting that systemic inflammation is currently thought to play a central role in the pathophysiology of cirrhosis and PH, and that the degree of systemic inflammation correlates with disease severity[41,42]. Cholestasis and circulatory congestion, if present, also increase liver stiffness[43–45], showing that LSM can sense different types of mechanical stimuli.

**Table 1 | Characteristics of patients included in the study**

| Variable | C ($n = 9$) | 1 DC ($n = 10$) | >1 DC ($n = 10$) | Total ($n = 29$) |
|---|---|---|---|---|
| **Age (years)** | 56.56 ± 7.51 | 51.9 ± 15.62 | 52.7 ± 7.243 | 53.62 ± 10.75 |
| **Sex: M/F (%)** | 33/67 | 40/60 | 50/50 | 41/59 |
| **Etiology: HCV/HBV/ARLD/MASH/others[$] (%)** | 56/11/0/22/11 | 40/10/0/0/50 | 10/10/50/10/20 | 34/10/17/10/28 |
| **CSPH: N/Y (%)** | 22/78 | 10/90 | 0/100 | 10/90 |
| **HVPG (mmHg)** | 14.5 ± 4.9 | 17.8 ± 6.5 | 20.3 ± 4.7(**) | 17.6 ± 5.8 |
| **HCC: N/Y (%)** | 100/0 | 100/0 | 100/0 | 100/0 |
| **Liver stiffness by VCTE (kPa)** | 26.92 ± 12.83 | 37.57 ± 20.31 | 53.55 ± 20.18(**) | 35.89 ± 19.13 |
| **Ascites: N/Y (%)** | 100/0 | 30/70 | 0/100 | 41/59 |
| **Hepatic encephalopathy: N/Y (%)** | 100/0 | 90/10 | 40/60 | 76/24 |
| **Esophageal variceal hemorrhage: N/Y (%)** | 100/0 | 80/20 | 80/20 | 86/14 |
| **Other decompensations: N/Y (%)** | 100/0 | 100/0 | 60/40 | 86/14 |
| **AST (U/L)** | 93 ± 80 | 80 ± 40 | 154 ± 112 | 110 ± 87 |
| **ALT (U/L)** | 78 ± 63 | 45 ± 22 | 58 ± 35 | 60 ± 43 |
| **GGT (U/L)** | 120 ± 140 | 53 ± 31 | 316 ± 272 | 160 ± 202 |
| **ALP (U/L)** | 439 ± 191 | 353 ± 155 | 408 ± 230 | 397 ± 189 |
| **INR** | 1.42 ± 0.48 | 1.58 ± 0.26 | 1.70 ± 0.51(*) | 1.57 ± 0.43 |
| **Bilirubin (mg/dL)** | 2.22 ± 3.26 | 2.97 ± 1.46(**) | 11.26 ± 12.03(**) | 5.72 ± 8.33 |
| **PLT (x10$^3$/uL)** | 129.60 ± 90.94 | 85.80 ± 32.57 | 146.80 ± 113 | 120.40 ± 86.66 |
| **Albumin (g/dL)** | 3.94 ± 1.31 | 3.12 ± 0.40(**) | 2.99 ± 0.43(**) | 3.29 ± 0.83 |
| **Na (mmol/L)** | 138.3 ± 4.41 | 139.8 ± 3.01 | 135.9 ± 6.33 | 138.0 ± 4.96 |
| **MELD** | 13 ± 11 | 15 ± 3 | 20 ± 8(*) | 16 ± 8 |
| **Child-Pugh class: A/B/C/NA (%)** | 67/11/0/22 | 0/60/40/0 | 0/20/80/0 | 21/31/41/7 |
| **FIB4 score** | 8.76 ± 9.28 | 8 ± 4.52 | 11.65 ± 13.19 | 9.49 ± 9.47 |
| **Relative ERG area (a.u.)** | 1.00 ± 0.27 | 1.09 ± 0.41 | 0.99 ± 0.17 | 1.03 ± 0.29 |

[$]Other etiologies are represented by autoimmune hepatitis, primary biliary cholangitis or primary sclerosing cholangitis. (**) statistically significantly different values compared to compensated patients, $p < 0.05$ (*) statistically significantly different values compared to compensated patients, $p < 0.1$.
Categorical variables are expressed in % and continuous variables in mean ± SD. Sample distributions were assessed for normality (Kolmogorov-Smirnov test). Normally distributed data were compared with unpaired Student t test or with Ordinary One-way ANOVA test. *M* male, *F* female, *HCV* hepatitis C virus, *HBV* hepatitis B virus, *ARLD* alcoholic liver disease, *MASH* non-alcoholic steatohepatitis, *CSPH* clinically significant portal hypertension, *HVPG* hepatic venous pressure gradient, *AST* aspartate aminotransferase, *ALT* alanine aminotransferase, *GGT* gamma-glutamyl transferase, *ALP* alkaline phosphatase, *INR* international normalized ration, *PLT* platelets, *MELD* model for end stage liver disease, *NA* missing data, *VCTE* vibration-controlled transient elastography.

Because of this and considering our in vitro findings demonstrating ERG downregulation in response to both stiffness and inflammation, we then extended our analysis to a larger cohort, including patients in different disease stages. Contrary to what we expected, we could not establish a relationship between disease stage or liver stiffness and degree of ERG downregulation. ALT levels did show a significant inverse correlation with ERG levels, which may indicate a connection between decreased ERG expression and liver inflammation. While in HUVECs increased stiffness showed a marked downregulation on ERG, inflammatory stimuli could significantly downregulate ERG under "healthy-like" stiffness conditions. This may suggest that in chronic liver disease, ERG is initially downregulated by inflammation and then further maintained by the increased stiffness. It is likely that the modulation of ERG in the context of CLD is multifactorial, and there are additional stimuli besides inflammation and stiffness which affect its expression, such as shear stress[46] or hypoxia[26], which may explain the profound downregulation at the mRNA level found in our transcriptomics dataset. In any case, our findings suggest that ERG downregulation in cirrhosis is a relatively early phenomenon, already maximally expressed in compensated patients, and not enhanced upon development of first or additional clinical decompensations. Furthermore, ERG downregulation was independent of the etiology of cirrhosis.

Furthermore, we investigated ERG levels in a $CCl_4$ rat model of CLD progression and regression. Previously, Dufton et al. demonstrated that ERG is strongly downregulated in a mouse model of $CCl_4$-induced liver injury, both in the acute and chronic setting[28]. Surprisingly, our rat model did not display any changes in ERG levels after 2 or 6 weeks of $CCl_4$ administration and only a mild downregulation at the full cirrhotic stage. This may be partly due to the experimental design since our model allows a recovery time of up to 1 week before sacrifice. During this time, the effects of acute inflammation may decrease or disappear and may allow for recovery of ERG expression. Moreover, as evidenced by the in vitro LSECs experiments, rat ECs seem to be less responsive in terms of ERG expression to underlying matrix stiffness as compared to human ECs. Taken together, our observations may suggest yet undescribed protective mechanisms of ERG expression in the rat liver.

Another interesting aspect of ERG biology worth mentioning in the context of cirrhosis is its relationship with epigenetic modifications. It has been shown in the context of lung disease that age- or bleomycin-induced chromatin changes affect ERG-binding loci, modulating endothelial phenotype and response to injury[24]. It is conceivable that these mechanisms may also play a role in the context of liver disease and mechanobiology, which are both intimately connected to epigenetic modifications.

Some limitations of our study are represented by the lack of in vitro studies using human LSECs, to clearly ascertain the responsiveness of ERG to stiffness and inflammation in another cell type besides HUVECs, which is a regularly used cell type in vascular biology- and ERG-related studies, as well as by the limited number of human samples.

ERG contributes to maintain vascular balance by countering inflammation and modulating angiogenesis in ECs. In this study we demonstrate that cirrhosis, characterized by increased stiffness and inflammation,

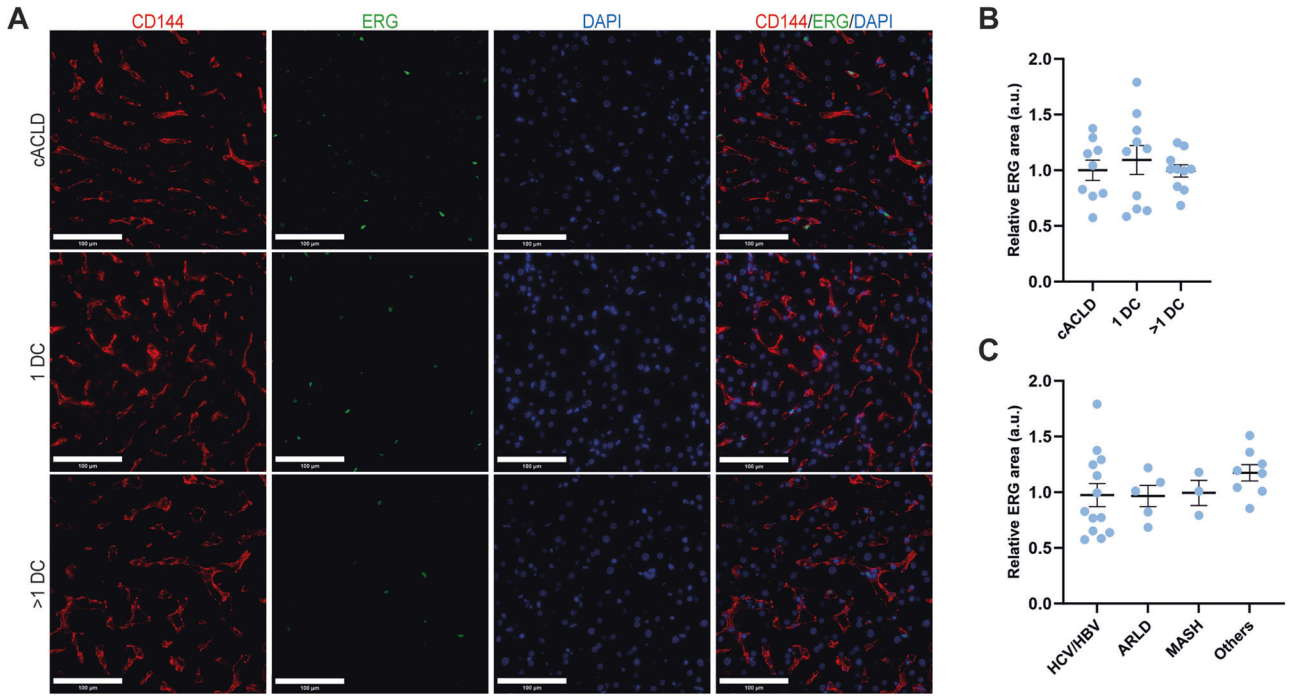


**Fig. 4 | ERG expression is independent of disease stage and etiology in cirrhosis.** **A** IF and **B** corresponding quantification of ERG (green) expression in human healthy and cirrhotic liver tissue from two independent cohorts of patients. CD144 (red) was used as marker for ECs. For each experiment, sample distributions were assessed for normality (Kolmogorov-Smirnov test). Normally distributed data were compared with unpaired Student t test or with Ordinary One-way ANOVA test. Non-significant p-values not displayed. CD144=cluster of differentiation 144, DAPI = 4′,6-diamidino-2-phenylindole, C compensated (disease), DC decompensation, HCV hepatitis C virus, HBV hepatitis B virus, ALD alcohol related liver disease, MASH metabolic dysfunction associated steatohepatitis, others autoimmune hepatitis, primary biliary cholangitis or primary sclerosing cholangitis, scale bar = 100 µm.

triggers ERG downregulation. By in vitro experiments, separating stiffness, and inflammatory response, we showed that stiffness appears dominant in driving ERG reduction, while inflammation gains importance under physiological stiffness. This interplay may suggest that inflammation downregulates ERG during the development of CLD, while increased stiffness becomes pivotal as CLD advances towards cirrhosis, regardless of disease etiology. These results enhance understanding of ERG's role in liver disease, suggesting that modulation of ERG may potentially have beneficial effects in cirrhosis and PH.

## Methods

### Human samples

Human tissue was obtained from explants or remnants from patients undergoing orthotopic liver transplantation (various etiologies) or surgery for excision of liver metastases or hydatid cysts at the Inselspital Bern (Kantonale Ethikkommission - KEK 2021-01403). Human liver samples from patients with histologically proven cirrhosis in different disease stages (compensated, decompensated with 1 decompensation or decompensated with more than 1 decompensation) were obtained from the "Octavian Fodor" Institute of Gastroenterology and Hepatology", Cluj-Napoca, Romania (Aviz IRGH nr 5735/2404.2023), from patients undergoing HVPG measurement and transjugular liver biopsy for diagnostic purposes. Biopsies were embedded in paraffin and 3 µm thickness slides were cut. Clinical data associated with liver biopsies was obtained, anonymized, from the informatic database. At the time of liver biopsy, all patients signed informed written consent allowing the use of their tissue and clinical/laboratory data as study material. The study was conducted in accordance with the protocol as approved by the Authorities, the Declaration of Helsinki, good clinical practice (GCP), the Human Research Act (HRA), the Human Research Ordinance (HRO) and all national, state, and local laws of the applicable regulatory agencies.

### Animals

Male and female Sprague Dawley rats were kept at the animal facilities of the University of Bern. Male Wistar Han rats were used at the animal facilities of the University of Barcelona Medical School. All animals were maintained in controlled environmental conditions with 12 h light-dark cycles and fed ad libitum with water and standard rodent food. All experiments were approved by the Bern Cantonal Ethics Committee and the Laboratory Animal Care (BE89/2021) and Use Committee of the University of Barcelona and were conducted under the European Community guidelines for the protection of animals used for experimental and other scientific purposes (EEC Directive 86/609).

### Induction of liver cirrhosis

Carbon tetrachloride ($CCl_4$) cirrhotic model was induced in male Wistar rats weighing 50–70 g by chronic $CCl_4$ inhalation (thrice per week) whilst receiving 0.3 g/L phenobarbital in the drinking water. Treatment was discontinued after 10 weeks, a timepoint at which animals would have developed cirrhosis, but not ascitic decompensation. This was followed by 1 week of rest period. Thioacetamide (TAA) cirrhotic model was induced in male and female Sprague Dawley rats weighing 250–300 g by injecting 200 mg/kg TAA (Sigma-Aldrich, Ref. No. 172502) i.p. twice a week for 12 weeks, followed by 1 week of rest period.

### Liver sinusoidal endothelial cells isolation

LSECs were isolated as previously described. Briefly, rats were anesthetized with ketamine + xylazine + midazolam (80 mg/kg – 10 mg/kg – 5 mg/kg, i.p) and laparotomy was performed. The livers were perfused twice through the portal vein with modified Hanks Balanced Salt Solution and digested with collagenase A (Sigma Aldrich-Roche #COLLA-RO). The resulting liver suspension was filtered through a 100-µm nylon cell strainer into ice-cold Krebs Solution and centrifuged for 5 min at 60 g. The supernatant contained

all non-parenchymal cells, while the pellet contained hepatocytes. LSEC and Kupffer cells were separated from HSCs by a three-step OptiPrep™ iodixanol gradient centrifugation (Sigma-Aldrich #D1556) and LSECs were finally separated from KCs by unspecific adhesion. Further details of the isolation procedure can be found in the original publication describing this protocol[47].

### Polyacrylamide gels

Polyacrylamide gels of 0.5 and 30 kPa were produced as previously described[4]. Briefly, round coverslips of 12- or 50-mm diameter were treated with an ethanol (Sigma Aldrich #1.00983), acetic acid (Sigma Aldrich #1.00063) and 3- (trimethoxysilyl)propyl methacrylate (Sigma Aldrich-Merck #440159) solution (14:1:1 ratio) for 30 minutes to activate the surfaces. Square coverslips of 22×22- or 60×60-mm were treated with Sigmacote (Sigma Aldrich-Merck #SL2) to create a hydrophobic layer. 2% bis-acrylamide (Bio-Rad #1610142) and 40% acrylamide (Bio-Rad #1610140) were mixed in PBS in different concentrations, with ammoniumpersulfate (Sigma Aldrich-Merck #A3678) and N,N,N′,N′-Tetramethylethylendiamin (TEMED) (Sigma Aldrich-Merck #T9281) to catalyze polymerisation, to obtain the desired stiffness. Different amounts of these solutions were applied to the square hydrophobic coverslips (depending on the size and desired thickness of the gel). The round-activated coverslips were then applied over to extend the solution and left to polymerise for 30 min. Following proper polymerisation, the hydrophobic square coverslip was removed, and a functionalisation solution composed of MilliQ $H_2O$, HEPES (Sigma Aldrich-Merck #H3375), Di-[1,1,1-tris-(hydroxymethyl)-propan]-tetraacrylat (Sigma Aldrich-Merck #408360) 0.2% in ethanol, α-Hydroxy-4-(2-hydroxyethoxy)-α-methylpropiophenon (Sigma Aldrich-Merck #410896) 5% in ethanol, N-(Acryloyloxy)-succinimid (Sigma Aldrich-Merck #A8060) 1% in dimethyl sulfoxide (Sigma Aldrich #D2650) and 0.2% bis-acrylamide (Bio-Rad #1610142) was applied on top and exposed to UV to ensure functionalization. After rinsing with HEPES and PBS, the gel was incubated with rat tail collagen type I (Sigma Aldrich-Merck #C3867) 0.1 mg/mL overnight. Gels were rinsed, UV-sterilized for 30 min, and incubated with cell growth medium for at least 1 h before use.

### Cells and cell treatments

HUVECs (Lonza #C2519A) were maintained in M199 medium (Thermo Fisher #12350039) supplemented with 20% fetal bovine serum (Thermo Fisher #10270106), 1% Antibiotic-Antimycotic Solution (Sigma Aldrich #A5955), 0.01% heparin (Sigma Aldrich #H3393) and 0.005% endothelial cell growth supplement (Sigma Aldrich-Merck #01-102). Freshly isolated LSECs were maintained in Roswell Park Memorial Institute medium 1640 (Thermo Fisher#21875034) supplemented with 10% fetal bovine serum, 1% Antibiotic-Antimycotic Solution, 0.01% heparin and 0.005% endothelial cell growth supplement. Inflammatory stimulation was done with 10 ng/mL IL1β in PBS. 12 h before treatments, cells were switched to serum-free medium. Time and concentration of treatment were chosen based on previous literature and our own preliminary experiments.

### Immunofluorescence analysis

Cells were fixed in 4% paraformaldehyde for 15 min, permeabilized with 0.1% Triton, and blocked with 1% BSA in PBS for 1 h at room temperature. Subsequently, overnight incubation with primary antibodies against ERG (1:500, Abcam #ab133264) and CD144 (1:500, Thermo-Fisher #14-1449-82) was done overnight at 4 °C. Secondary antibody incubation was performed with Goat Anti-Rabbit IgG H&L (Alexa Fluor® 488) (Abcam #ab150077) and Goat Anti-Mouse IgG H&L (Cy5 ®) (Abcam #ab6563) in combination with DAPI for 1 h at room temperature. Preparations were then mounted with Fluorescence Mounting Medium (Agilent Dako #S302380-2) and dried overnight. Four-6 images were obtained per slide and per channel at 63× magnification for LSECs and 40× magnification for HUVECs with a Leica DM400B microscope. Image analysis of fluorescence was performed using ImageJ software and fluorescence intensities were normalized by number of cells per field. Formalin-fixed paraffin-embedded tissue slides from human or rat livers were deparaffinized in xylol and hydrated with ethanol. Heat-mediated antigen retrieval was performed in Tris-EDTA solution and blocking was done with 5% goat serum for 1 h at room temperature. Subsequently, overnight incubations with primary antibodies against ERG (1:500, Abcam #ab133264) and CD144 (1:500, Thermo-Fisher #14-1449-82) were done overnight at 4 °C. Secondary antibody incubation was performed with Goat Anti-Rabbit IgG H&L Alexa Fluor® 488 (1:300, Abcam #ab150077) and Goat Anti-Mouse IgG H&L Cy5 ® (1:1000, Abcam #ab6563) in combination with DAPI for 1 h at room temperature. Tissue autofluorescence was quenched with Vector® TrueVIEW® Autofluorescence Quenching Kit (Vector Laboratories #SP-8400-15). Preparations were then mounted with Fluorescence Mounting Medium (Agilent Dako #S302380-2) and dried overnight. Four-six images were obtained per slide and per channel at 40× magnification with a Leica DM400B microscope. Image analysis of fluorescence was performed using ImageJ software and fluorescence area was normalized by total area of the image (area of expression/$cm^2$ tissue) in a blinded manner.

### Western Blot

Cells on polyacrylamide gels were trypsinised, centrifuged and lysed in RIPA Buffer. Protein concentrations were determined using the Pierce™ BCA Protein Assay Kit (Thermo Scientific #23225). Protein extracts were boiled in reducing sample buffer (Thermo-Fisher #39000) at 95 °C for 5 min. A total of 5–10 µg samples were separated by sodium dodecyl sulfate-polyacrylamide gel electrophoresis (SDS-PAGE) in 12% acrylamide gels. Proteins were then transferred onto nitrocellulose membranes, which were blocked with 5% non-fat milk in TBST for 60 min at room temperature, washed 3 times with TBST and incubated overnight at 4 °C with primary antibody against ERG (1:200, Santa Cruz, #sc-526021) and 1 hour at room temperature with HRP-conjugated secondary antibody (1:2000, Santa Cruz, #sc-526021). HRP conjugated anti-GAPDH antibody (1:5000, Abcam #ab185059) was used for loading control.

### Real-time quantitative PCR

RNA was isolated and purified using the RNeasy Mini Kit (Qiagen, #74104), according to manufacturer protocol. RNA concentration was measured using Nanodrop spectrophotometer and retro-transcription to cDNA was performed using the Quantitect Reverse Transcription Kit (Qiagen, #205311). RT-PCR was performed using the TaqMan Fast Universal PCR Master Mix (Applied Biosystems, #4352042) and predesigned TaqMan probes in a QuantStudio 5 Real-time-PCR-System.

### Bioinformatic analysis

A preliminary gene network expansion was undertaken using Enrichr, a tool developed by the Ma'ayan lab (https://maayanlab.cloud/Enrichr/), employing the ARCHS4 RNA-seq gene-gene co-expression matrix. This approach aimed to pinpoint genes exhibiting co-expression patterns with ERG[48,49]. Network expansion was further analyzed by Reactome or GO process including the top 10 genes related with the pre-expanded list (https://maayanlab.cloud/enrichr-kg). To predict ERG-related pathways and biological processes, we utilized (ARCHS4) (https://maayanlab.cloud/archs4/)[50]. Datasets pertaining to HUVECs and human LSECs (GSE164799, GSE18401, and GSE32984, respectively) were accessed from the GEO repository. After filtering both HUVECs database with human LSECs for common DEGs, the resulting list was subject to GSEA Hallmark as well as Panther Pathway analysis to observe functional classification (https://www.pantherdb.org/).

### Statistical analysis

Statistical analysis was performed using GraphPad Prism 6 (GraphPad Software, CA, USA). Data represent biological replicates (n) and were depicted as mean values ± standard error (SEM). Frequency distribution of data was assessed with Normality test (Kolmogorov-Smirnov). For samples characterized by a normal distribution, means were compared by Student t-test (2 samples), or ANOVA ( > 2 samples) followed by the Tukey post-

hoc analysis. Non-parametric tests (Kruskal-Wallis) followed by Mann-Whitney U test were used otherwise. Differences were considered significant at $p < 0.05$.

Received: 14 March 2024; Accepted: 19 July 2024;
Published online: 01 October 2024

## References

1. Gracia-Sancho, J., Marrone, G. & Fernández-Iglesias, A. Hepatic microcirculation and mechanisms of portal hypertension. *Nat. Rev. Gastroenterol. Hepatol.* **16**, 221–234 (2019).
2. Gracia-Sancho, J., Caparrós, E., Fernández-Iglesias, A. & Francés, R. Role of liver sinusoidal endothelial cells in liver diseases. *Nat. Rev. Gastroenterol. Hepatol.* **18**, 411–431 (2021).
3. Felli, E. et al. Mechanobiology of portal hypertension. *JHEP Rep.* **5**, 100869 (2023).
4. Guixé-Muntet, S. et al. Nuclear deformation mediates liver cell mechanosensing in cirrhosis. *JHEP Rep.* **2**, 100–145 (2020).
5. Greuter, T. et al. Mechanotransduction-induced glycolysis epigenetically regulates a CXCL1-dominant angiocrine signaling program in liver sinusoidal endothelial cells in vitro and in vivo. *J. Hepatol*. (Published online April 12, 2022).
6. Mambetsariev, I. et al. Stiffness-activated GEF-H1 expression exacerbates LPS-induced lung inflammation. *PLoS ONE* **9**, e92670 (2014).
7. Stroka, K. M. & Aranda-Espinoza, H. Endothelial cell substrate stiffness influences neutrophil transmigration via myosin light chain kinase-dependent cell contraction. *Blood* **118**, 1632–1640 (2011).
8. Andreu, I. et al. Mechanical force application to the nucleus regulates nucleocytoplasmic transport. *Nat. Cell Biol.* **24**, 896–905 (2022).
9. Gracia-Sancho, J. et al. Endothelial expression of transcription factor Kruppel-like factor 2 and its vasoprotective target genes in the normal and cirrhotic rat liver. *Gut* **60**, 517–524 (2011).
10. Marrone, G. et al. KLF2 exerts antifibrotic and vasoprotective effects in cirrhotic rat livers: behind the molecular mechanisms of statins. *Gut* **64**, 1434–1443 (2015).
11. Guixé-muntet, S. et al. Cross-talk between autophagy and KLF2 determines endothelial cell phenotype and microvascular function in acute liver injury. *J. Hepatol.* **66**, 86–94 (2017).
12. Marrone, G. et al. The transcription factor KLF2 mediates hepatic endothelial protection and paracrine endothelial–stellate cell deactivation induced by statins. *J. Hepatol.* **58**, 98–103 (2013).
13. Elosegui-Artola, A. et al. Force triggers YAP nuclear entry by regulating transport across nuclear pores. *Cell* **171**, 1397–1410.e14 (2017).
14. Miralles, F., Posern, G., Zaromytidou, A. I. & Treisman, R. Actin dynamics control SRF activity by regulation of its coactivator MAL. *Cell* **113**, 329–342 (2003).
15. Shah, A. V., Birdsey, G. M. & Randi, A. M. Regulation of endothelial homeostasis, vascular development and angiogenesis by the transcription factor ERG. *Vasc. Pharm.* **86**, 3–13 (2016).
16. Adamo, P. & Ladomery, M. R. The oncogene ERG: a key factor in prostate cancer. *Oncogene* **35**, 403–414 (2015).
17. Tsuzuki, S., Taguchi, O. & Seto, M. Promotion and maintenance of leukemia by ERG. *Blood* **117**, 3858–3868 (2011).
18. Yuan, L. et al. Anti-inflammatory effects of the ETS factor ERG in endothelial cells are mediated through transcriptional repression of the interleukin-8 gene. *Circ. Res* **104**, 1049 (2009).
19. Dryden, N. H. et al. The transcription factor Erg controls endothelial cell quiescence by repressing activity of nuclear factor (NF)-κB p65. *J. Biol. Chem.* **287**, 12331–12342 (2012).
20. Sperone, A. et al. The transcription factor Erg inhibits vascular inflammation by repressing NF-kappaB activation and proinflammatory gene expression in endothelial cells. *Arterioscler Thromb. Vasc. Biol.* **31**, 142–150 (2011).
21. Peghaire, C. et al. The transcription factor ERG regulates a low shear stress-induced anti-thrombotic pathway in the microvasculature. *Nat. Commun.* **10**, 1–17 (2019).
22. Birdsey, G. M. et al. The transcription factor Erg regulates expression of histone deacetylase 6 and multiple pathways involved in endothelial cell migration and angiogenesis. *Blood* **119**, 894–903 (2012).
23. Yuan, L. et al. RhoJ is an endothelial cell-restricted Rho GTPase that mediates vascular morphogenesis and is regulated by the transcription factor ERG. *Blood* **118**, 1145–1153 (2011).
24. Caporarello, N. et al. Dysfunctional ERG signaling drives pulmonary vascular aging and persistent fibrosis. *Nat. Commun.* **13**, 4170 (2022).
25. Lathen, C. et al. ERG-APLNR axis controls pulmonary venule endothelial proliferation in pulmonary veno-occlusive disease. *Circulation* **130**, 1179–1191 (2014).
26. Looney, A. P. et al. Synergistic role of endothelial ERG and FLI1 in mediating pulmonary vascular homeostasis. *Am. J. Respir. Cell Mol. Biol.* **57**, 121–131 (2017).
27. Schafer, C. M. et al. Cytokine-Mediated Degradation of the Transcription Factor ERG Impacts the Pulmonary Vascular Response to Systemic Inflammatory Challenge. *Arterioscler Thromb Vasc Biol*. 43:0-00. https://doi.org/10.1161/ATVBAHA.123.318926 (2023).
28. Dufton, N. P. et al. Dynamic regulation of canonical TGFβ signalling by endothelial transcription factor ERG protects from liver fibrogenesis. *Nat. Commun.* **8**, 1–14 (2017).
29. Gan, W. et al. SPOP promotes ubiquitination and degradation of the ERG oncoprotein to suppress prostate cancer progression. *Mol. Cell* **59**, 917–930 (2015).
30. Wang, S. et al. The ubiquitin ligase TRIM25 targets ERG for degradation in prostate cancer. *Oncotarget* **7**, 64921–64931 (2016).
31. Shah, A. V. et al. The endothelial transcription factor ERG mediates Angiopoietin-1-dependent control of Notch signalling and vascular stability. *Nat. Commun.* **8**, 16002 (2017).
32. Manicardi, N. et al. Transcriptomic profiling of the liver sinusoidal endothelium during cirrhosis reveals stage-specific secretory signature. *Cancers (Basel).* **13**, 2688 (2021).
33. Killaars, A. R. et al. Extended exposure to stiff microenvironments leads to persistent chromatin remodeling in human mesenchymal stem cells. *Adv. Sci.* **6**, 1801483 (2019).
34. Caliari, S. R. et al. Gradually softening hydrogels for modeling hepatic stellate cell behavior during fibrosis regression. *Integr. Biol. (Camb.)* **8**, 720 (2016).
35. Guixé-Muntet, S., Quesada-Vázquez, S. & Gracia-Sancho, J. Pathophysiology and therapeutic options for cirrhotic portal hypertension. *Lancet Gastroenterol Hepatol.* **9**, 646–663 (2024).
36. Yang, L. et al. Vascular endothelial growth factor promotes fibrosis resolution and repair in mice. *Gastroenterology* **146**, 1339–1350.e1 (2014).
37. de Franchis, R. et al. Baveno VII – Renewing consensus in portal hypertension. *J. Hepatol.* **76**, 959–974 (2022).
38. Berzigotti, A. Non-invasive evaluation of portal hypertension using ultrasound elastography. *J. Hepatol.* **67**, 399–411 (2017).
39. Arena, U. et al. Acute viral hepatitis increases liver stiffness values measured by transient elastography. *Hepatology* **47**, 380–384 (2008).
40. Coco, B. et al. Transient elastography: a new surrogate marker of liver fibrosis influenced by major changes of transaminases. *J. Viral Hepat.* **14**, 360–369 (2007).
41. Arroyo, V. et al. The systemic inflammation hypothesis: towards a new paradigm of acute decompensation and multiorgan failure in cirrhosis. *J. Hepatol.* **74**, 670–685 (2021).
42. Costa, D. et al. Systemic inflammation increases across distinct stages of advanced chronic liver disease and correlates with decompensation and mortality. *J. Hepatol.* **74**, 819–828 (2021).
43. Berzigotti, A. et al. Effect of meal ingestion on liver stiffness in patients with cirrhosis and portal hypertension. *PLoS ONE* **8**, e58742 (2013).

44. Millonig, G. et al. Extrahepatic cholestasis increases liver stiffness (FibroScan) irrespective of fibrosis. *Hepatology* **48**, 1718–1723 (2008).
45. Millonig, G. et al. Liver stiffness is directly influenced by central venous pressure. *J. Hepatol.* **52**, 206–210 (2010).
46. Schafer, C. M. et al. An inhibitor of endothelial ETS transcription factors promotes physiologic and therapeutic vessel regression. *Proc. Natl Acad. Sci. USA* **117**, 26494–26502 (2020).
47. Fernández-Iglesias, A., Ortega-Ribera, M., Guixé-Muntet, S. & Gracia-Sancho, J. 4 in 1: Antibody-free protocol for isolating the main hepatic cells from healthy and cirrhotic single rat livers. *J. Cell Mol. Med.* **23**, 877–886 (2019).
48. Chen, E. Y. et al. Enrichr: Interactive and collaborative HTML5 gene list enrichment analysis tool. *BMC Bioinf.* **14**, 1–14 (2013).
49. Kuleshov, M. V. et al. Enrichr: a comprehensive gene set enrichment analysis web server 2016 update. *Nucleic Acids Res.* **44**, W90–W97 (2016).
50. Lachmann, A. et al. Massive mining of publicly available RNA-seq data from human and mouse. *Nat. Commun*. **9** https://doi.org/10.1038/S41467-018-03751-6 (2018).


## Acknowledgements

This study was carried out at the Department of Biomedical Research at the University of Bern and at the Esther Koplowitz Center, Institut d'Investigacions Biomèdiques August Pi i Sunyer in Barcelona. Funders of this study had no role in study design, data collection and analysis, decision to publish, or preparation of the paper. We are indebted to Philipp Kellmann, Carlos Wotzkow and Dr. Bobe Petrushev for technical support. We acknowledge the Translational Research Unit at the Institute of Pathology, University of Bern, Switzerland, for excellent technical support and Tissue Bank Bern (TBB) for providing the human tissue samples.

## Author contributions

S.-E.S. and E.F. equally contributed to the manuscript S.-E.S.: Conceptualization, Methodology, Investigation, Writing. E.F.: Conceptualization, Methodology, Investigation, Writing. C.W.: Methodology, Investigation, Writing. Y.N.: Methodology, Investigation. J.J.L.: Software, Validation, Formal analysis. S.G.-M.: Conceptualization, Investigation, Formal analysis. H.Ş.: Conceptualization, Resources, Writing. J.B.: Conceptualization, Methodology, Writing, Supervision, Funding acquisition. A.B.: Conceptualization, Methodology, Writing, Supervision, Funding acquisition. J.G.-S.: Conceptualization, Methodology, Writing, Supervision, Funding acquisition.

## Competing interests

J.B. is a consultant for Astra-Zeneca, Boehringer-Ingelheim, Novo-Nordisk, and Resolution Therapeutics. A.B. is a consultant for Boehringer-Ingelheim.

## Additional information

**Supplementary information** The online version contains supplementary material available at https://doi.org/10.1038/s44355-024-00007-7.

**Correspondence** and requests for materials should be addressed to Jordi Gracia-Sancho.